ACS OMEGA

http://pubs.acs.org/journal/acsodf

Article

Highly Sensitive and Reliable microRNA Detection with a Recyclable Microfluidic Device and an Easily Assembled SERS Substrate

Taeksu Lee, Soongeun Kwon, Hak-Jong Choi, Hyungjun Lim, and Jaejong Lee*

Cite This: *ACS Omega* 2021, 6, 19656−19664

Read Online

ACCESS | Metrics & More | Article Recommendations | Supporting Information

ABSTRACT: Surface-enhanced Raman spectroscopy (SERS) detection in microfluidics is an interesting topic because of its high sensitivity, miniaturization, and ability to perform online detection. However, the difficulties in generating SERS-based microfluidic devices with uniform signal reproducibility and high sensitivity have hindered their widespread application. In addition, the recyclability of the SERS-based microfluidic devices can contribute to their broad commercialization, but the possible contamination in the detection area and cumbersome cleaning procedures remain a challenge. In this study, we describe a repeatable SERS-based microfluidic device comprising a disposable SERS substrate and a reusable microfluidic channel. The microfluidic channel was prepared via mechanical processing, and the SERS substrate was fabricated by nanoimprint lithography and electrodeposition. The SERS substrate and microfluidic channel can be attached easily because they were assembled using screws. The SERS substrate achieved an excellent SERS enhancement factor greater than 10^8 over a large sample area, signal uniformity, and substrate-to-substrate reproducibility. This guaranteed reliable and sensitive signals in every experiment. Furthermore, the disposable SERS substrate contributed exact detection of target molecules. Finally, their practical application was demonstrated with the repeated use of the microfluidic device by detecting a specific micro-RNA, (miR-34a) at a concentration as low as 5 fM.

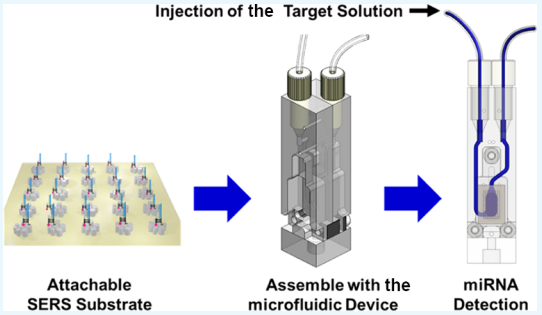

1. INTRODUCTION

Surface-enhanced Raman spectroscopy (SERS) measurements coupled with microfluidic devices have several advantages in conventional macro-environments because they are molecular specific analytical tools with high sensitivity (to a single molecular level). For instance, by combining SERS with microfluidic devices, researchers can miniaturize their laboratory setup for SERS quantification. This would allow the quantification of trace amounts of the target molecules in the microliter range of reagents, control the movement of particles in channels, decrease the assay time and number of procedures required, and offer portability.[1−6]

A notable approach for realizing this SERS-based microfluidic system entails the use of colloidal metallic nanomaterials as sensing elements, which are mixed with the sensing target analytes in the fluidic channel. However, their Raman response reproducibility is extremely poor owing to the difficulty in creating uniform SERS-active sites. This is because the colloidal metal nanoparticles have to be injected into the channel at a controlled flow rate, and the microfluidic chip design in such systems has to be elaborate.[1,7−9]

Another approach involves the fabrication of metal nanostructure arrays in microfluidic channels, such as direct laser writing or growing metal nanostructures inside the channel. Although they exhibit improved signal uniformity, their sensitivities are usually lower than those of colloidal nanoparticles because it is difficult to generate narrow nanogaps between metal nanostructures. In addition, they often require complex instruments and time-consuming synthetic steps, such as multiple lithography and etching, metal deposition, stacking, and bonding of glass substrates.[1,4,10]

Moreover, manufacturing SERS-microfluidic devices for a one-time use is expensive, which limits their utility. These problems also extend to the application of other microfluidic technologies and are not specific to SERS-based microfluidic chips.[11−13] However, problems that arise during the repeated use of microfluidic devices, such as the possible false-positive signal caused by the contamination of the detection area (i.e., the remaining molecules on the metal nanostructures) and cumbersome cleaning steps, should be simultaneously addressed to enable their broad commercial applications. Therefore, it is envisaged that the combination of disposable, ultra-sensitive, and reliable SERS substrates along with reusable microfluidic channels can offer unique advantages, thereby

Received: May 3, 2021
Accepted: June 22, 2021
Published: July 21, 2021

Scheme 1. (a) Schematic Design of a Repeatable SERS-Based Microfluidic Device[a]

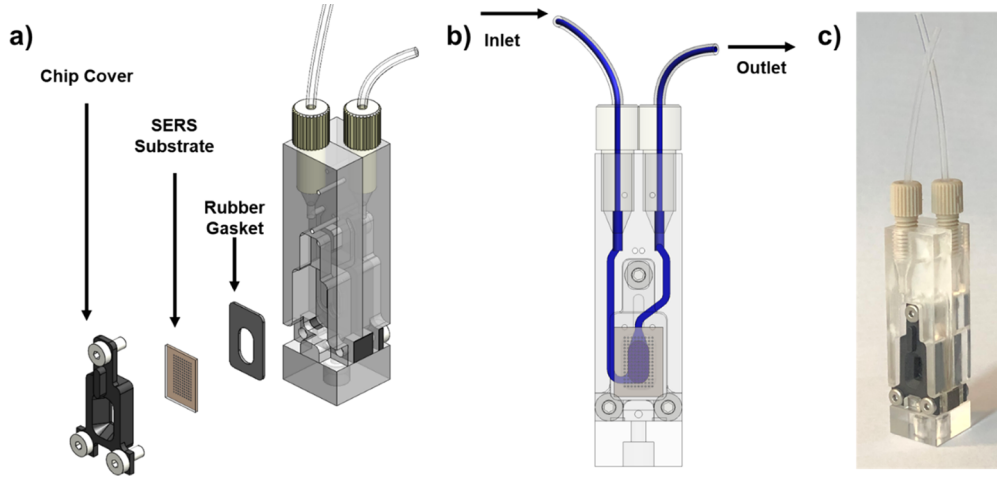

[a]Highly sensitive and reliable SERS substrates were fabricated through nanoimprint lithography and an electrodeposition process, and miR-34a-specific MB was modified on the surface of the SERS substrate. The fabricated SERS substrate was assembled with screws on the microfluidic device. (b) Cross-section view of the device to display the microfluidic channel. (c) SERS-based microfluidic device.

Scheme 2. (a) Fabrication Procedure for Fabricating SERS Substrates through Nanoimprint Lithography and an Electrodeposition Process[a]

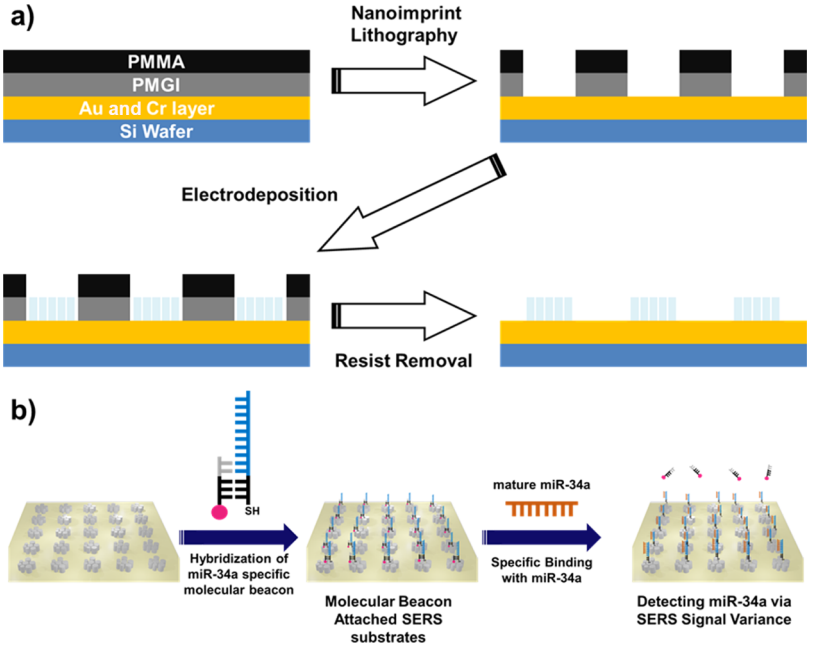

[a]After synthesis, PMMA and PMGI, as a template, were removed by wet etching with an excess amount of acetone and AZ-MIF 300. (b) Schematic illustration of the MB-based SERS analysis for miR-34a detection. First, the miR-34a-specific MBs were attached onto the SERS substrate via Ag−S bonding. The MB configuration was disrupted in the presence of miR-34a, leading to the detachment of the Cy3-labeled portion from the SERS substrate owing to the hybridization with the target miR-34a and finally leading to a variation in the SERS intensity.

opening up new opportunities in various fields of research.[14−17]

Herein, we present a recyclable SERS-based microfluidic device that comprises a disposable SERS substrate and reusable microfluidic channel (Scheme 1). The microfluidic channel was prepared via mechanical processing, and the SERS substrate was synthesized using nanoimprint lithography and electrodeposition.[18−20] The microfluidic channel and SERS substrate were assembled with screws; therefore, they could be easily attached and detached. The produced SERS substrate displayed high sensitivity [an enhancement factor (EF) greater than 10^8], signal uniformity over a large area (a relative standard deviation of 10.7 ± 1.87%), and good substrate-to-substrate reproducibility, thereby ensuring a reliable and sensitive signal in the recurrent experiment. Moreover, the disposable SERS substrate was able to avoid false signals that may be caused by the residues left on the metal nanostructure array with repeated use.[14−17]

To demonstrate the practical application of our SERS microfluidic device, miR-34a, a type of miRNA, was repeatedly detected using the microfluidic device while changing the SERS substrate in every experiment. Although miR-34a is a

https://doi.org/10.1021/acsomega.1c02306
ACS Omega 2021, 6, 19656−19664

well-known biomarker in the fields of medical diagnosis and treatment because of its special role as a suppressor of tumor genes or oncogenes, the detection of the biomarker itself has been restricted by its low abundance and structural instability.[18,21−23] To specifically recognize miR-34a, the surface of the SERS substrate was modified with an miR-34a-specific molecular beacon (MB), and the MB-modified SERS substrate was assembled into the microfluidic device. Based on the repeated use of the device, both good reproducibility and selective detection of the experiment were confirmed. Furthermore, extremely low concentrations of miR-34a (as low as 5 fM) were also detected.

2. RESULTS AND DISCUSSION

The fabrication process of a highly sensitive and reliable SERS microfluidic channel device was designed for repeated use. The process comprises the following three major steps: first, disposable SERS substrates with evenly distributed narrow nanogaps over the entire dices are manufactured by nanoimprint lithography and a successive electrodeposition process under a relatively high overpotential (−3 V vs Ag/AgCl) (Scheme 2a). The second step is the modification of SERS substrates with an miR-34a-specific MB (Scheme 2b). The final stage is the formation of a reusable microfluidic channel mounting the SERS substrate on the cover of the microfluidic device and tightening/untightening the cover using the screws.[24] When the solution is injected into the microfluidic device through the inlet, the void volume in the lower part of the device is filled and the SERS substrate recognizes the target analytes in the solution. Then, the SERS substrate is unscrewed from the microfluidic device and analyzed via Raman spectroscopy. The separated microfluidic device is then rinsed at least three times with a buffer solution or distilled water, and another SERS substrate is attached to the microfluidic device for further use. Scheme 1c illustrates the integrated microfluidic device assembly with a disposable SERS substrate.

Figures 1a, S2, and S3 show the representative scanning electron microscopy (SEM) images of the SERS substrates after removing the nanoimprint resist using an excess amount of acetone and the AZ-MIF 300 developer.[25] It is apparent that the silver nanostructures were successfully deposited, with several small nanogaps between them that covered the entire surface of the wafer. The mean diameter of the silver nanostructures was estimated using the ImageJ program and found to be approximately 514 ± 20 nm. The relatively high overpotential (−3 V vs Ag/AgCl) resulted in a rapid growth of multiple silver nanostructures. Furthermore, energy-dispersive X-ray spectrometry (EDX) analysis confirmed the distribution of Ag on the SERS substrates (Figure S4). The silver nanostructures were generated only inside the nanoholes because the bottom part of the nanoholes was exposed to the silver precursors, whereas the outer parts of the nanoholes were blocked by the non-conductive nanoimprint resist.[18] An attempt without the nanohole pattern yielded irregularly shaped silver nanostructures, and no nanogaps were generated (Figure S5). These small nanogaps contributed to the boosting of the signal in the Raman spectra after the rhodamine 6G (R6G) target molecules were loaded (Figure 1b). X-ray diffraction (XRD) studies were also performed to confirm the highly crystalline structure of the fabricated SERS substrates (Figure 1c).[26−28] Furthermore, X-ray photoelectron spectra (XPS) demonstrated successful silver deposition after the electrodeposition process. Figure 1d,e represents the Au 4f and Ag 3d orbitals at a high resolution. Two dominating gold signals (87.4 and 83.7 eV), corresponding to the Au $4f_{5/2}$ and Au $4f_{7/2}$ orbitals, exist in the nanohole pattern. The binding energy difference between the doublet peaks was 3.7 eV with an intensity ratio of 4:3, which can be indexed to Au^0. Some signals for gold were also observed in the SERS substrates; this can be attributed to the presence of the gold atoms outside the silver nanostructures. However, their signal intensities were much lower than those of the nanohole pattern. In contrast, the doublet peaks of Ag $3d_{3/2}$ and $3d_{5/2}$, centered at 373 and 367 eV, respectively, with an intensity ratio of 2:3 in the SERS substrates, denote silver in its zero-valent form, Ag^0, whereas no silver signal was detected in the nanohole pattern as expected.[29,30] These results support the claim that the resulting enhancement in the Raman signal of the SERS substrates was due to the presence of silver on the surface.

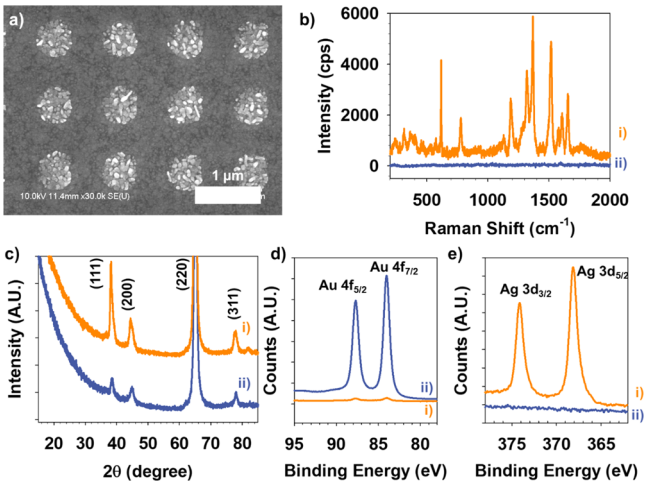

Figure 1. (a) Representative SEM image of SERS substrates. (b) Raman spectra of (i) SERS substrate and (ii) nanohole pattern after 10^{-6} M of R6G treatment. (c) XRD spectra and high-resolution (d) Au 4f and (e) Ag 3d X-ray photoelectron spectra of (i) SERS substrate and (ii) nanohole pattern.

Our proposed microfluidic system employs a reusable microfluidic channel and disposable SERS substrate for sensing target materials, that is, a new SERS substrate was installed in the device for every experiment. Therefore, reliable signal reproducibility and ultra-sensitivity are the most important prerequisites. High signal amplification capability should be uniformly maintained over a wide area and for each new substrate.

We first demonstrated the high signal uniformity of the fabricated SERS substrate after loading 1×10^{-6} M of R6G and obtained Raman mapping images (Figure 2a) as well as the intensities of their characteristic vibration bands at 1360 and 1508 cm^{-1} (C−C ring stretching in the xanthene ring) and 1648 cm^{-1} (C−C stretching in the xanthene ring) (Figure 2b).[31] The Raman mapping image was recorded on an 8 μm × 8 μm area based on a Raman signal intensity at 1648 cm^{-1}. The brightness in these images was uniform, which confirmed the excellent reproducibility of the fabricated SERS substrate. We selected representative Raman peaks of R6G at 1360, 1508, and 1648 cm^{-1} to further investigate the uniformity of the Raman spectra. The relative standard deviation (RSD) of intensity was measured to be 10.7 ± 1.87%, indicating an excellent signal reproducibility for continuous detection. We

https://doi.org/10.1021/acsomega.1c02306
ACS Omega 2021, 6, 19656−19664

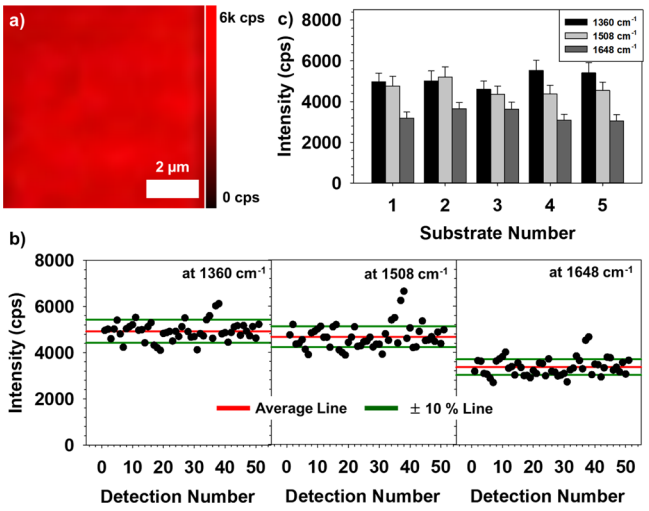

Figure 2. (a) Raman mapping image over 8 μm × 8 μm of the SERS substrate after R6G (10^{-6} M) M treatment. It displays a Raman signal intensity of approximately 1648 cm^{-1}, the distinct Raman peak of R6G. (b) Raman signal intensity distribution at 1360, 1508, and 1648 cm^{-1} from (a). (c) Synthetic reproducibility data of the SERS substrate. The peak intensities of 10^{-6} M R6G were measured from 5 SERS substrates from different synthetic batches.

also confirmed a good substrate-to-substrate reproducibility of the SERS signal by obtaining the RSD (7.85 ± 0.84%) of the average SERS intensities at 1360, 1508, and 1648 cm^{-1} of five SERS substrates fabricated from five different batches (Figure 2c). The Raman intensities of R6G (10^{-6} M) on the silver nanostructure slightly diminished after a week; this indicated the long-term stability of the substrate (Figure S8).

R6G, as a probe molecule, was then detected at ultra-low concentrations of 10^{-13}, 10^{-12}, 10^{-11}, and 10^{-10} M using a 785 nm excitation laser to examine the capability of the SERS substrate. Figure 3 exhibits sharp, well-resolved, and enhanced characteristic Raman bands of R6G even at a concentration of 10^{-13} M [limit of detection (LOD)]. The SERS intensities gradually decreased with respect to the diluted R6G solutions. In addition, the SERS EF of the SERS substrate was further calculated using the same molecules. The regular Raman signal of 10^{-4} M of R6G on a bare gold-coated Si wafer was first measured, and its signal intensity was compared to that of 10^{-13} M of the R6G-treated SERS substrate (Figure S9). The calculated EF value was approximately 2.14 × 10^{8}, and this signal boost stemmed from several small nanogaps between the silver nanostructures on the SERS substrate. Compared to the method using colloidal nanoparticles, this synthesized SERS substrate presented excellent signal uniformity over large areas and substrate-to-substrate reproducibility. Furthermore, the present methodology manifested highly improved signal enhancement and convenience of synthesis, unlike other methods for fabricating metal nanostructure arrays in closed microfluidic channels, such as the direct laser writing method. Hence, it can be concluded that the fabricated SERS substrates exhibit promising potential for producing reliable signals in the repeated experiments of our microfluidic device.

We performed further experiments to detect miRNAs using our microfluidic system, which has been considered a key biomarker, owing to its close association with their expression patterns and certain disease types or stages. Among them, miR-34a was selected because it assists in regulating various biological functions, such as cellular differentiation, proliferation, metastasis, and apoptosis.[32−34] However, the detection of miRNAs has often been limited by their low abundance in the total RNA samples and the sophisticated profiling of miRNAs. Because of the instability caused by their short structure, miRNAs are easily destroyed in the middle of the detection process, which makes their sensing difficult. This implies that the accurate detection of small amounts of the miRNA samples within a short time is important. Therefore, the SERS-based microfluidic detection system can be the most appropriate candidate for detecting miRNAs owing to its ability to detect small amounts of samples at extremely low concentrations within a short reaction time.[35−37]

Prior to detection, we modified the surface of the SERS substrate with miR-34a-specific MB, and two types of linear oligonucleotides were prepared. One type was able to recognize miR-34a from its complementary structure and was bonded with the Cy3 dye at the end. The other type was shorter oligonucleotides, conjugated with thiol groups at the end of the attachment on the SERS substrate. These two types of oligonucleotides were annealed together to form MB. MB was hybridized with the SERS substrate through a salt-aging process, and distinct Cy3 peaks on the SERS substrate after modification with MB manifested successful attachment (Figure S11).[18,38,39] These MB-immobilized SERS substrates were assembled into the microfluidic channel by fixing the chip cover with screws.

The recyclability of our disposable SERS substrate-assembled microfluidic device was first explored by repeatedly detecting the same concentration of miR-34a. Prior to the experiment, we tested the most optimal condition to detect miR-34a (Figures S12 and S13) and determined that the

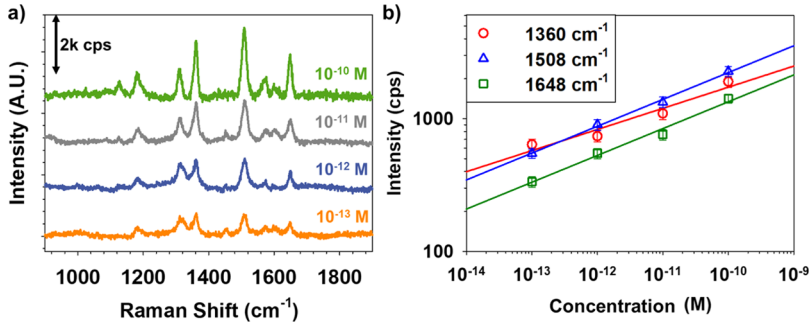

Figure 3. (a) SERS spectra of the fabricated SERS substrate loaded with R6G of analyte concentrations ranging from 10^{-13} to 10^{-10} M. (b) Calibration curve of Raman intensity at cm^{-1} in Figure 3a against different logarithmic R6G concentrations.

https://doi.org/10.1021/acsomega.1c02306
ACS Omega 2021, 6, 19656−19664

detection of miR-34a at 37 °C for 1 h was the most appropriate condition. First, 50 pM of miR-34a solution was injected into the microfluidic channel and stored at 37 °C for 1 h. After the reaction, the SERS substrate was detached from the device for the measurement. A new MB-modified SERS substrate was reassembled on the device, and the miR-34a samples with identical concentrations were injected again under the same conditions. This cycle was repeated five times, and the corresponding Raman spectra of each SERS substrate are shown in Figure 4. This graph clearly demonstrates that similar

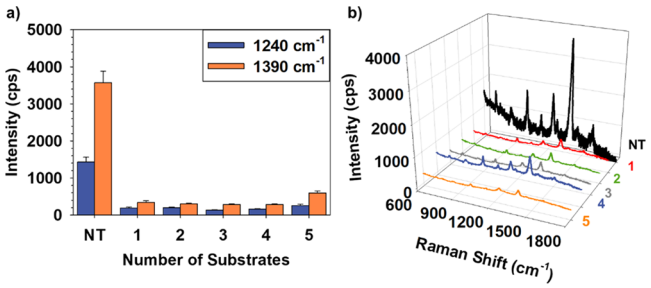

Figure 4. (a) Repeated detection of 5 pM miR-34a with the same microfluidic device while the SERS substrates were changed upon every detection time. (b) Representative Raman spectra of the SERS substrate during repeated detection of 5 pM miR-34a after washing the microfluidic device and reunion with the MB-modified SERS substrate. Analysis of the SERS substrate was performed using a 785 nm laser at 50 mW for 10 s.

signal strength was produced when the same concentration of miR-34a was reacted during the repeated experiments, thereby illustrating the outstanding recyclability of our proposed microfluidic device. The wide application of SERS-based microfluidic devices has been restricted to date by their lack of reusability. This is because the residues of the target materials or probe molecules on the metal nanostructures may cause contamination when the devices are used to detect different species. However, in this system, the contamination problem was resolved by changing the new SERS substrate every time an experiment was performed; therefore, the reusability property can significantly promote the utilization and lower the manufacturing cost of the microfluidic device.[40,41]

The performance of a reusable microfluidic device with disposable SERS substrates was further evaluated using various types of miR-34a concentrations. The same microfluidic device was used repeatedly by changing only the SERS substrate. After the reaction, the cy3 signal on MB was detached from the SERS substrate because of the hybridization between the miR-34a molecules and MB. This affected the thermodynamic equilibrium state of MB by the variation in the length of the binding site. The larger binding sites between miR-34a and MB resulted in a more stable and preferred hybridization than that of the previous thiol-labeled oligonucleotides, when constructing another duplex structure.[32] Consequently, the Cy3 signal on the SERS substrate decreased gradually as the concentration of miR-34a increased from 5 fM to 5 pM (Figures 5a and S14). The LOD in micro-RNA was determined by the value that was not smaller than the standard deviation of the control group, so the LOD value of miR-34a was 5 fM. In addition, other types of miRNAs (miR-34b and miR-34c) with relatively high concentrations (5 pM) were injected into the microfluidic device, and their SERS spectra were obtained. Figures 5b and S15 demonstrate that there is no significant variation in the signal intensity after the injection of miR-34b and miR-34c, whereas the signal intensity decreased greatly after the injection of miR-34a at the same concentration. Therefore, a microfluidic device with miR-34a-specific MB-modified SERS substrates enabled the selective recognition of the specific target analytes with low LODs in practical biomedical applications.

Reliable detection of micro-RNA in biological samples is an important prerequisite for practical sensor applications. We further prepared different concentrations of miR-34a in serum solution (10% serum in the buffer solution), and the proposed SERS microfluidic device was utilized to detect miR-34a under serum conditions. Figure 6 displays the Raman intensity of Cy3 peaks varied with respect to the concentration of miR-34a in the serum solution. Unfortunately, the LOD value in plasma exceeded the LOD value in the pure buffer solution owing to the complexity in the serum sample. Nevertheless, this result supported that the presented SERS microfluidic channel could detect micro-RNA in the real biological sample.

3. CONCLUSIONS

This study demonstrated a reliable, highly sensitive, and repeatable SERS-based microfluidic system comprising detachable SERS substrates. Highly sensitive and reproducible SERS substrates were fabricated via nanoimprint lithography and an electrodeposition process, whereas the microfluidic device was fabricated via mechanical processing. The SERS substrates exhibited excellent substrate-to-substrate reproducibility and Raman signal enhancement, as high as 10^8, with excellent

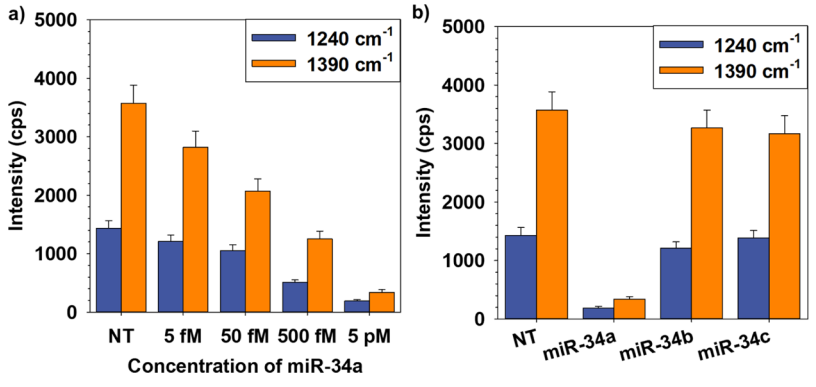

Figure 5. (a) Detection of different concentrations of miR-34a (5 fM to 5 pM) and (b) different types of miRNAs using a similar microfluidic device, whereas SERS substrates were replaced after every measurement.

https://doi.org/10.1021/acsomega.1c02306
ACS Omega 2021, 6, 19656−19664

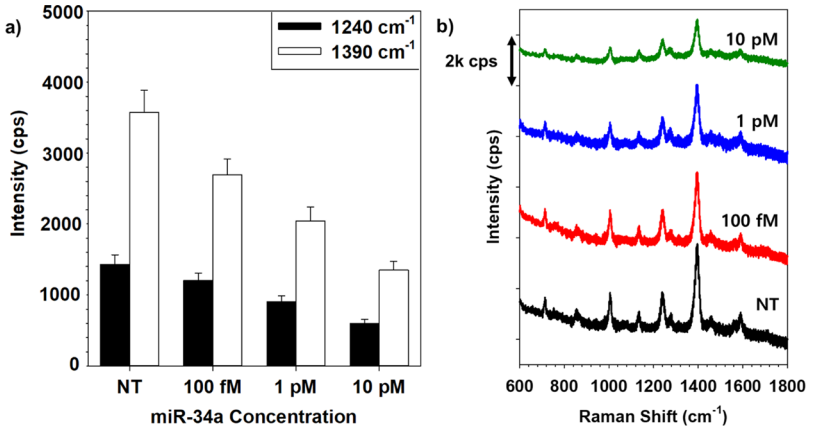

Figure 6. (a) Average peak intensities of miR-34a MB on SERS substrates in the microfluidic device at 1240 and 1390 cm^{-1} after detection of various concentrations of target miR-34a in the serum solution (10% serum in the buffer solution). (b) Representative Raman spectra of the MB-modified SERS substrate after the treatment of the various concentrations of target miR-34a in the serum-contained solution with a microfluidic device. Analysis of the SERS substrate was performed using a 785 nm laser at 50 mW for 10 s.

signal uniformity. After surface modification with the miR-34a-specific MB, the SERS substrates were assembled into the microfluidic device with screws. Therefore, repeatable detection of the target analyte was possible by washing the microfluidic device thoroughly and replacing the disposable SERS substrate with a new substrate in every experiment. These replaceable SERS substrates contributed toward solving the contamination problem caused by the residues of the target molecules on the metal nanostructures. Considering the capabilities of this reusable SERS-based microfluidic device, it has the potential to be developed as a powerful sensing tool for addressing the emerging requirements in biomedical applications, food safety evaluation, and environmental monitoring.

4. MATERIALS AND METHODS

4.1. Fabrication of the Microfluidic Devices. The microfluidic device comprises a disposable SERS substrate and reusable channel. The device was fabricated by mechanical processing designed using the SolidWorks software. The main body of the microfluidic device comprises transparent polycarbonate. The specific dimensions of the microfluidic channel were as follows: width = 1000 μm, depth = 500 μm, and length = 43.9 mm. The upper part of the main body was connected to a tap to fit a tube such that the liquid could flow in or out of the channel. The disposable substrate and reusable channel can be simply assembled and disassembled by mounting the SERS substrate on the cover of the microfluidic device and tightening/untightening the cover using the screws. By attaching the rubber gasket to the microfluidic device, the air gap between the SERS substrate and device can be removed to prevent solvent leakage. The volume of the SERS substrate-mounted room was 21.3 μL, whereas the minimum volume for filling the microchannel was 63.1 μL.

4.2. Preparation of the Nanohole Pattern. A thin Cr layer (5 nm) and Au layer (50 nm) were deposited onto the Si wafers via E-beam lithography. Then, polymethylglutarimide (PMGI SF3, MicroChem Corp., USA) and a thermal nanoimprint resist (mr-I 8010R, Microresist Technology GmbH, Germany) were spin-coated (3000 rpm, 30 s) and baked at 200 and 100 °C for 5 min and 3 min, respectively. The wafer with the double layer was subjected to thermal nanoimprinting under a pressure of 50 bar for 4 min at 200 °C using a commercial tool (ANT-6HO3, KIMM, Korea) and pillar-patterned silicon stamp (480 nm in diameter, a 1000 nm pitch) as the master mold.

After the nanohole pattern was generated, the residues of the thermal nanoimprint resist were etched using O_2 plasma, and the remaining PMGI was removed by wet etching with a commercial developer solution (AZ-MIF300, AZ Electronic Materials, Germany) for 3 s. Finally, the nanohole pattern was diced to 8 × 12 mm^2 to be assembled into the microfluidic device.

4.3. Fabrication of SERS Substrates and Modification with miR-34a-Specific MB. The SERS substrates were manufactured by depositing silver nanoarrays inside the nanohole pattern. Briefly, the dices with the nanohole pattern and bare Au coated Si wafers acted as the working electrodes. The non-reactive areas of the dices were passivated using non-conducting pastes to enhance the efficiency of electrodeposition. Electrochemical deposition was performed using a potentiostat (CompactStat, Ivium) with a conventional three-electrode system [Pt wire counter electrode and a Ag/AgCl (3 M KCl) reference electrode]. Silver deposition solution (0.5 mM) was prepared by dissolving the silver precursor in distilled water (DI) with sodium carbonate. Silver nanoarrays were fabricated by applying −3 V (vs Ag/AgCl) for 30 s at room temperature. After electrodeposition, the polymer resist was removed using an excess amount of acetone (OCI, Korea) and the AZ-MIF300 developer. The morphology of the SERS substrates was analyzed by field-emission SEM (S-4800, Hitachi, Japan). The C, O, N, Ag, and Au signals of the SERS substrates were detected using EDX (HORIBA, Japan). The average diameter of the silver nanostructures was determined using the ImageJ program. The crystal structure of the SERS substrates was analyzed by X-ray diffraction (Ultima3 Diffractometer, Rigaku) at room temperature, and the surface elemental information of the SERS substrates was obtained using X-ray photoelectron spectrometry (K-alpha, Thermo U. K.) with a monochromatic $Al_{K\alpha}$ X-ray source.

We prepared two types of oligomers (Bioneer Inc., Daejeon, Korea), the sequences of which were as follows: 5′-HS-TTC GCT GTA CAA CCA GCT AAG ACA CTG CCA-3′ and 3′-Cy3-GCG ACA TGT TG-5′. These oligomers were mixed with the same molar ratios and annealed at 95 °C for 4 min

https://doi.org/10.1021/acsomega.1c02306
ACS Omega 2021, 6, 19656−19664

and thereafter at 70 °C for 10 min. Finally, the samples were slowly cooled to room temperature.

4.4. SERS Measurements and EF Calculations. We prepared various concentrations of R6G solution (10^{-13} to 10^{-6} and 10^{-3} M) in ethanol. The fabricated substrates were immersed in each solution for 4 h and then dried overnight. The Raman spectra were recorded via confocal Raman microscopy (LabRAM ARAMIS, HORIBA). A diode laser operating at 785 nm was used as the excitation source with a laser power of approximately 50 mW; the integration time was 10 s, and the laser diameter was 2 μm. A silicon wafer with a Raman band at 520 cm^{-1} was used as the reference for calibration. We used the LabSpec 5 software (HORIBA) for spectral and image processing, analysis, and baseline correction. R6G was purchased from Sigma-Aldrich, Korea.

To calculate the SERS EF values, we prepared a Au thin film (50 nm)-covered Si wafer as a reference. The analytical SERS EF for the R6G molecules on the SERS substrates was estimated using eq 1

$$EF = (I_{SERS}/I_{dye}) \times (C_{dye}/C_{SERS}) \quad (1)$$

where C_{dye} is the concentration of R6G treated on the bare Au substrate (1×10^{-3} M), C_{SERS} is the concentration of R6G treated on the surface of the SERS substrates (10^{-12} M), I_{dye} is the signal intensity of the R6G Raman spectra on the pure Au substrate after treatment with 10^{-3} M R6G solution, and I_{SERS} is the signal intensity of the R6G Raman spectra on the surface of the SERS substrates after treatment with the 10^{-12} M R6G solution.

4.5. Hybridization of the MB to the SERS Substrates. The miR-34a-specific MB was mixed with 100 times the high molar ratio of tris(2-carboxyethyl)phosphine (Sigma-Aldrich, Korea) overnight. The produced SERS substrates were immersed in 0.6 mL of 0.1 μM MB solution. Then, four aliquots of 2 M NaCl (10 mM Tris) solution (0.05 M, two times; 0.1 M, two times) were added to the adjusted solution to obtain a solution of 0.3 M NaCl. They were stored at 4 °C overnight and washed thrice with phosphate-buffered saline (PBS).

4.6. Detection of miR-34a with the Microfluidic Devices. To detect miR-34a using the microfluidic device, 100 μL of various concentrations of miR-34a (5 fM to 5 pM) solutions was prepared in reaction buffers (10 mM Tris-HCl, 100 mM KCl, and 1 mM $MgCl_2$, pH 8.0), and each solution was injected into the device. The microfluidic device was stored at 37 °C for 1 h. For optimization, the reactions were conducted at 4 and 37 °C. We also stored the device for 20 min, 1 h, and 4 h at 37 °C. After the reaction, the SERS substrate was detached from the microfluidic device, washed with PBS, and analyzed using Raman spectroscopy (LabRAM ARAMIS, HORIBA). The microfluidic device was washed twice with the incubation buffer and once with DI for further use. Then, a new SERS substrate, hybridized with MB, was attached to the device, and the solutions of different miR-34a concentrations were injected for repeated detection.

For comparison, 5 pM miR-34b and miR-34c samples were also analyzed using identical procedures.

■ ASSOCIATED CONTENT

Supporting Information

The Supporting Information is available free of charge at https://pubs.acs.org/doi/10.1021/acsomega.1c02306.

FE-SEM images, EDX analysis, overall XPS spectra, Raman mapping results without the Raman reporter, Raman spectra for EF calculations, confirmation of resist removal, beacon hybridization, synthetic uniformity, and stability (PDF)

■ AUTHOR INFORMATION

Corresponding Author

Jaejong Lee − *Department of Nano Manufacturing Technology, Korea Institute of Machinery and Materials (KIMM)^{RINGGOLD}, Daejeon 34103, Republic of Korea;* orcid.org/0000-0001-7684-2667; Email: jjlee@kimm.re.kr

Authors

Taeksu Lee − *Department of Nano Manufacturing Technology, Korea Institute of Machinery and Materials (KIMM)^{RINGGOLD}, Daejeon 34103, Republic of Korea;* orcid.org/0000-0002-8245-7148

Soongeun Kwon − *Department of Nano Manufacturing Technology, Korea Institute of Machinery and Materials (KIMM)^{RINGGOLD}, Daejeon 34103, Republic of Korea*

Hak-Jong Choi − *Department of Nano Manufacturing Technology, Korea Institute of Machinery and Materials (KIMM)^{RINGGOLD}, Daejeon 34103, Republic of Korea;* orcid.org/0000-0002-8080-9998

Hyungjun Lim − *Department of Nano Manufacturing Technology, Korea Institute of Machinery and Materials (KIMM)^{RINGGOLD}, Daejeon 34103, Republic of Korea;* orcid.org/0000-0003-3769-8046

Complete contact information is available at: https://pubs.acs.org/10.1021/acsomega.1c02306

Author Contributions

The manuscript was written through contributions of all authors. All authors have given approval to the final version of the manuscript.

Notes

The authors declare no competing financial interest.

■ ACKNOWLEDGMENTS

This research was supported by BioNano Health-Guard Research Center funded by the Ministry of Science and ICT(MSIT) of Korea as the Global Frontier Project (grant number H-GUARD_2013M3A6B2078943).

■ REFERENCES

(1) Bai, S.; Serien, D.; Hu, A.; Sugioka, K. 3D microfluidic Surface-Enhanced Raman Spectroscopy (SERS) chips fabricated by all-femtosecond-laser-processing for real-time sensing of toxic substances. *Adv. Funct. Mater.* **2018**, *28*, 1706262.

(2) Jeon, J.; Choi, N.; Chen, H.; Moon, J.-I.; Chen, L.; Choo, J. SERS-based droplet microfluidics for high-throughput gradient analysis. *Lab Chip* **2019**, *19*, 674−681.

(3) Li, X.; Yuan, G.; Yu, W.; Xing, J.; Zou, Y.; Zhao, C.; Kong, W.; Yu, Z.; Guo, C. A self-driven microfluidic surface-enhanced Raman scattering device for Hg 2+ detection fabricated by femtosecond laser. *Lab Chip* **2020**, *20*, 414−423.

(4) Mendl, A.; Köhler, J. M.; Boskovic, D.; Löbbecke, S. Novel SERS-based process analysis for label-free segmented flow screenings. *Lab Chip* **2020**, *20*, 2364.

(5) Reza, K. K.; Sina, A. A. I.; Wuethrich, A.; Grewal, Y. S.; Howard, C. B.; Korbie, D.; Trau, M. A SERS microfluidic platform for targeting

multiple soluble immune checkpoints. *Biosens. Bioelectron.* **2019**, *126*, 178−186.
(6) Ying, B.; Park, S.; Chen, L.; Dong, X.; Young, E. W. K.; Liu, X. NanoPADs and nanoFACEs: an optically transparent nanopaper-based device for biomedical applications. *Lab Chip* **2020**, *20*, 3322−3333.
(7) Ge, T.; Yan, S.; Zhang, L.; He, H.; Wang, L.; Li, S.; Yuan, Y.; Chen, G.; Huang, Y. Nanowire assisted repeatable DEP−SERS detection in microfluidics. *Nanotechnology* **2019**, *30*, 475202.
(8) Sun, D.; Cao, F.; Cong, L.; Xu, W.; Chen, Q.; Shi, W.; Xu, S. Cellular heterogeneity identified by single-cell alkaline phosphatase (ALP) via a SERRS-microfluidic droplet platform. *Lab Chip* **2019**, *19*, 335−342.
(9) Ramalingam, S.; Chand, R.; Singh, C. B.; Singh, A. Phosphorene-gold nanocomposite based microfluidic aptasensor for the detection of okadaic acid. *Biosens. Bioelectron.* **2019**, *135*, 14−21.
(10) Zhou, Q.; Kim, T. Review of microfluidic approaches for surface-enhanced Raman scattering. *Sens. Actuators, B* **2016**, *227*, 504−514.
(11) Sun, H.; Chan, C.-W.; Wang, Y.; Yao, X.; Mu, X.; Lu, X.; Zhou, J.; Cai, Z.; Ren, K. Reliable and reusable whole polypropylene plastic microfluidic devices for a rapid, low-cost antimicrobial susceptibility test. *Lab Chip* **2019**, *19*, 2915−2924.
(12) Saez, J.; Glennon, T.; Czugala, M.; Tudor, A.; Ducreé, J.; Diamond, D.; Florea, L.; Benito-Lopez, F. Reusable ionogel-based photo-actuators in a lab-on-a-disc. *Sens. Actuators, B* **2018**, *257*, 963−970.
(13) Tang, J.; Guo, H.; Zhao, M.; Liu, W.; Chou, X.; Zhang, B.; Xue, C.; Zhang, W.; Liu, J. Ag nanoparticles cladded with parylene for high-stability microfluidic surface-enhanced Raman scattering (SERS) biochemical sensing. *Sens. Actuators, B* **2017**, *242*, 1171−1176.
(14) Erkal, J. L.; Selimovic, A.; Gross, B. C.; Lockwood, S. Y.; Walton, E. L.; McNamara, S.; Martin, R. S.; Spence, D. M. 3D printed microfluidic devices with integrated versatile and reusable electrodes. *Lab Chip* **2014**, *14*, 2023−2032.
(15) Guo, F.; Xie, Y.; Li, S.; Lata, J.; Ren, L.; Mao, Z.; Ren, B.; Wu, M.; Ozcelik, A.; Huang, T. J. Reusable acoustic tweezers for disposable devices. *Lab Chip* **2015**, *15*, 4517−4523.
(16) Cho, H.; Kim, J.; Jeon, C.-W.; Han, K.-H. A disposable microfluidic device with a reusable magnetophoretic functional substrate for isolation of circulating tumor cells. *Lab Chip* **2017**, *17*, 4113−4123.
(17) Zhao, S.; Wu, M.; Yang, S.; Wu, Y.; Gu, Y.; Chen, C.; Ye, J.; Xie, Z.; Tian, Z.; Bachman, H.; Huang, P.-H.; Xia, J.; Zhang, P.; Zhang, H.; Huang, T. J. A disposable acoustofluidic chip for nano/microparticle separation using unidirectional acoustic transducers. *Lab Chip* **2020**, *20*, 1298−1308.
(18) Lee, T.; Wi, J.-S.; Oh, A.; Na, H.-K.; Lee, J.; Lee, K.; Lee, T. G.; Haam, S. Highly robust, uniform and ultra-sensitive surface-enhanced Raman scattering substrates for microRNA detection fabricated by using silver nanostructures grown in gold nanobowls. *Nanoscale* **2018**, *10*, 3680−3687.
(19) Lee, T.; Jung, S.; Kwon, S.; Kim, W.; Park, J.; Lim, H.; Lee, J. Formation of Interstitial Hot-Spots Using the Reduced Gap-Size between Plasmonic Microbeads Pattern for Surface-Enhanced Raman Scattering Analysis. *Sensors* **2019**, *19*, 1046.
(20) Lee, T.; Kwon, S.; Jung, S.; Lim, H.; Lee, J.-J. Macroscopic Ag nanostructure array patterns with high-density hotspots for reliable and ultra-sensitive SERS substrates. *Nano Res.* **2019**, *12*, 2554−2558.
(21) Su, J.; Wang, D.; Nörbel, L.; Shen, J.; Zhao, Z.; Dou, Y.; Peng, T.; Shi, J.; Mathur, S.; Fan, C.; Song, S. Multicolor gold−silver nano-mushrooms as ready-to-use SERS probes for ultrasensitive and multiplex DNA/miRNA detection. *Anal. Chem.* **2017**, *89*, 2531−2538.
(22) Song, C. Y.; Yang, Y. J.; Yang, B. Y.; Sun, Y. Z.; Zhao, Y. P.; Wang, L. H. An ultrasensitive SERS sensor for simultaneous detection of multiple cancer-related miRNAs. *Nanoscale* **2016**, *8*, 17365−17373.
(23) Pang, Y.; Wang, C.; Wang, J.; Sun, Z.; Xiao, R.; Wang, S. Fe3O4@ Ag magnetic nanoparticles for microRNA capture and duplex-specific nuclease signal amplification based SERS detection in cancer cells. *Biosens. Bioelectron.* **2016**, *79*, 574−580.
(24) Jung, D.; Ahn, J.; Jo, N.; Lee, J.; Shin, Y.-B.; Lim, H. Cuvette-based microfluidic device integrated with nanostructures for measuring dual Localized Surface Plasmon Resonance (LSPR) signals. *Rev. Sci. Instrum.* **2018**, *89*, 113107.
(25) Wi, J.-S.; Park, J.; Kang, H.; Jung, D.; Lee, S.-W.; Lee, T. G. Stacked gold nanodisks for bimodal photoacoustic and optical coherence imaging. *ACS Nano* **2017**, *11*, 6225−6232.
(26) Lee, T.; Bang, D.; Chang, Y. W.; Choi, Y.; Park, K. Y.; Oh, A.; Han, S.; Kim, S. H.; Lee, K.; Suh, J.-S.; Huh, Y.-M.; Haam, S. Cancer theranosis using mono-disperse, mesoporous gold nanoparticles obtained via a robust, high-yield synthetic methodology. *RSC Adv.* **2016**, *6*, 13554−13561.
(27) Bang, D.; Chang, Y. W.; Park, J.; Lee, T.; Park, J.; Yeo, J.-S.; Kim, E.-K.; Yoo, K.-H.; Huh, Y.-M.; Haam, S. One-step electrochemical fabrication of vertically self-organized silver nanograss. *J. Mater. Chem. A* **2013**, *1*, 4851−4857.
(28) Lee, T.; Lim, J.; Park, K.; Lim, E.-K.; Lee, J. Peptidoglycan-binding Protein Metamaterials Mediated Enhanced and Selective Capturing of Gram-Positive Bacteria and their Specific, Ultra-sensitive, and Reproducible detection via SERS. *ACS Sens.* **2020**, *5*, 3099.
(29) Lee, T.; Kwon, S.; Lee, J. Highly Dense and Accessible Nanogaps in Au-Ag Alloy Patterned Nanostructures for Surface-Enhanced Raman Spectroscopy Analysis. *ACS Appl. Nano Mater.* **2020**, *6*, 5920.
(30) Lee, T.; Jung, D.; Wi, J.-S.; Lim, H.; Lee, J.-J. Surfactant-free galvanic replacement for synthesis of raspberry-like silver nanostructure pattern with multiple hot-spots as sensitive and reproducible SERS substrates. *Appl. Surf. Sci.* **2020**, *505*, 144548.
(31) Lamberti, A.; Virga, A.; Chiadò, A.; Chiodoni, A.; Bejtka, K.; Rivolo, P.; Giorgis, F. Ultrasensitive Ag-coated TiO 2 nanotube arrays for flexible SERS-based optofluidic devices. *J. Mater. Chem. C* **2015**, *3*, 6868−6875.
(32) Kim, E.; Yang, J.; Park, J.; Kim, S.; Kim, N. H.; Yook, J. I.; Suh, J.-S.; Haam, S.; Huh, Y.-M. Consecutive targetable smart nanoprobe for molecular recognition of cytoplasmic microRNA in metastatic breast cancer. *ACS Nano* **2012**, *6*, 8525−8535.
(33) Calin, G. A.; Croce, C. M. MicroRNA signatures in human cancers. *Nat. Rev. Canc.* **2006**, *6*, 857−866.
(34) He, L.; Hannon, G. J. MicroRNAs: small RNAs with a big role in gene regulation. *Nat. Rev. Genet.* **2004**, *5*, 522−531.
(35) Guo, S.; Lin, W. N.; Hu, Y.; Sun, G.; Phan, D.-T.; Chen, C.-H. Ultrahigh-throughput droplet microfluidic device for single-cell miRNA detection with isothermal amplification. *Lab Chip* **2018**, *18*, 1914−1920.
(36) Cheng, H.-L.; Fu, C.-Y.; Kuo, W.-C.; Chen, Y.-W.; Chen, Y.-S.; Lee, Y.-M.; Li, K.-H.; Chen, C.; Ma, H.-P.; Huang, P.-C.; Wang, Y.-L.; Lee, G.-B. Detecting miRNA biomarkers from extracellular vesicles for cardiovascular disease with a microfluidic system. *Lab Chip* **2018**, *18*, 2917−2925.
(37) Roy, S.; Soh, J. H.; Gao, Z. A microfluidic-assisted microarray for ultrasensitive detection of miRNA under an optical microscope. *Lab Chip* **2011**, *11*, 1886−1894.
(38) Li, J.; Zhu, B.; Zhu, Z.; Zhang, Y.; Yao, X.; Tu, S.; Liu, R.; Jia, S.; Yang, C. J. Simple and rapid functionalization of gold nanorods with oligonucleotides using an mPEG-SH/Tween 20-assisted approach. *Langmuir* **2015**, *31*, 7869−7876.
(39) Gill, R.; Göeken, K.; Subramaniam, V. Fast, single-step, and surfactant-free oligonucleotide modification of gold nanoparticles using DNA with a positively charged tail. *Chem. Commun.* **2013**, *49*, 11400−11402.
(40) Roman, J.; Français, O.; Jarroux, N.; Patriarche, G.; Pelta, J.; Bacri, L.; Le Pioufle, B. Solid-state nanopore easy chip integration in a cheap and reusable microfluidic device for ion transport and polymer conformation sensing. *ACS Sens.* **2018**, *3*, 2129−2137.
(41) Qiang, L.; Vaddiraju, S.; Rusling, J. F.; Papadimitrakopoulos, F. Highly sensitive and reusable Pt-black microfluidic electrodes for

https://doi.org/10.1021/acsomega.1c02306
ACS Omega 2021, 6, 19656−19664

long-term electrochemical sensing. *Biosens. Bioelectron.* **2010**, *26*, 682−688.

https://doi.org/10.1021/acsomega.1c02306
ACS Omega 2021, 6, 19656−19664